Loss of the BMP antagonist USAG-1 ameliorates disease in a mouse model of the progressive hereditary kidney disease Alport syndrome

Mari Tanaka, … , Toru Kita, Motoko Yanagita

Research Article   Nephrology

The glomerular basement membrane (GBM) is a key component of the filtering unit in the kidney. Mutations involving any of the collagen IV genes (*COL4A3*, *COL4A4*, and *COL4A5*) affect GBM assembly and cause Alport syndrome, a progressive hereditary kidney disease with no definitive therapy. Previously, we have demonstrated that the bone morphogenetic protein (BMP) antagonist uterine sensitization–associated gene-1 (USAG-1) negatively regulates the renoprotective action of BMP-7 in a mouse model of tubular injury during acute renal failure. Here, we investigated the role of USAG-1 in renal function in *Col4a3⁻/⁻* mice, which model Alport syndrome. Ablation of Usag1 in *Col4a3⁻/⁻* mice led to substantial attenuation of disease progression, normalization of GBM ultrastructure, preservation of renal function, and extension of life span. Immunohistochemical analysis revealed that USAG-1 and BMP-7 colocalized in the macula densa in the distal tubules, lying in direct contact with glomerular mesangial cells. Furthermore, in cultured mesangial cells, BMP-7 attenuated and USAG-1 enhanced the expression of MMP-12, a protease that may contribute to GBM degradation. These data suggest that the pathogenetic role of USAG-1 in *Col4a3⁻/⁻* mice might involve crosstalk between kidney tubules and the glomerulus and that inhibition of USAG-1 may be a promising therapeutic approach for the treatment of Alport syndrome.

Find the latest version:

https://jci.me/39569/pdf

Loss of the BMP antagonist USAG-1 ameliorates disease in a mouse model of the progressive hereditary kidney disease Alport syndrome

Mari Tanaka,[1] Misako Asada,[2] Atsuko Y. Higashi,[1] Jin Nakamura,[2] Akiko Oguchi,[2]
Mayumi Tomita,[3] Sachiko Yamada,[1] Nariaki Asada,[2] Masayuki Takase,[2] Tomohiko Okuda,[4]
Hiroshi Kawachi,[5] Aris N. Economides,[6] Elizabeth Robertson,[7] Satoru Takahashi,[8] Takeshi Sakurai,[9]
Roel Goldschmeding,[10] Eri Muso,[11] Atsushi Fukatsu,[3] Toru Kita,[1] and Motoko Yanagita[1,2,3]

[1]Department of Cardiovascular Medicine, [2]Career-Path Promotion Unit for Young Life Scientists,
[3]Department of Artificial Kidneys, and [4]COE Formation, Graduate School of Medicine, Kyoto University, Kyoto, Japan.
[5]Department of Cell Biology, Institute of Nephrology, Niigata University Graduate School of Medical and Dental Sciences, Niigata, Japan.
[6]Regeneron Pharmaceuticals Inc., Tarrytown, New York. [7]Wellcome Trust Center for Human Genetics, University of Oxford, Oxford, United Kingdom.
[8]Laboratory Animal Resource Center, Institute of Basic Medical Sciences, University of Tsukuba, Ibaraki, Japan. [9]Department of Molecular Neuroscience and
Integrative Physiology, Graduate School of Medical Science, Kanazawa University, Kanazawa, Japan. [10]Department of Pathology,
University Medical Center Utrecht, Utrecht, Netherlands. [11]Division of Nephrology and Dialysis, Department of Medicine, Kitano Hospital, Osaka, Japan.

The glomerular basement membrane (GBM) is a key component of the filtering unit in the kidney. Mutations involving any of the collagen IV genes (*COL4A3*, *COL4A4*, and *COL4A5*) affect GBM assembly and cause Alport syndrome, a progressive hereditary kidney disease with no definitive therapy. Previously, we have demonstrated that the bone morphogenetic protein (BMP) antagonist uterine sensitization–associated gene-1 (USAG-1) negatively regulates the renoprotective action of BMP-7 in a mouse model of tubular injury during acute renal failure. Here, we investigated the role of USAG-1 in renal function in *Col4a3*$^{-/-}$ mice, which model Alport syndrome. Ablation of Usag1 in *Col4a3*$^{-/-}$ mice led to substantial attenuation of disease progression, normalization of GBM ultrastructure, preservation of renal function, and extension of life span. Immunohistochemical analysis revealed that USAG-1 and BMP-7 colocalized in the macula densa in the distal tubules, lying in direct contact with glomerular mesangial cells. Furthermore, in cultured mesangial cells, BMP-7 attenuated and USAG-1 enhanced the expression of MMP-12, a protease that may contribute to GBM degradation. These data suggest that the pathogenetic role of USAG-1 in *Col4a3*$^{-/-}$ mice might involve crosstalk between kidney tubules and the glomerulus and that inhibition of USAG-1 may be a promising therapeutic approach for the treatment of Alport syndrome.

Introduction

The renal glomerular basement membrane (GBM) contributes importantly to maintenance of the structural integrity of the glomerular capillaries (1, 2). Type IV collagen is the major component of the GBM, and its mutations have been linked to the genetic disorder Alport syndrome, a progressive hereditary kidney disease associated with sensorineural deafness (3). With a genetic frequency of about 1 in 5,000 people, it counts among the more prevalent of known genetic disorders (4). The disease is caused by the mutations in any one of the genes encoding the α3, α4, and α5 chains of type IV collagen (*COL4A3*, *COL4A4*, and *COL4A5*) (5–7), and a mutation affecting 1 of these chains forming the α3/α4/α5(IV) collagen network can alter or abolish the GBM expression not only of the corresponding chain but also of the other 2 chains (8). The GBM in Alport syndrome instead retains the fetal α1/α1/α2(IV) collagen network (9), which confers an increased susceptibility to proteolytic enzyme, leading to progressive destruction of the GBM with subsequent hematuria and proteinuria, glomerulosclerosis and ultimately end-stage renal disease. The current therapy is

limited to dialysis and transplantation, with a higher risk of anti-GBM disease in the transplanted organs due to immune reaction against the type IV collagen chains.

Bone morphogenetic protein–7 (BMP-7) is a promising candidate to treat Alport syndrome. BMP-7 belongs to the TGF-β superfamily (10), and the kidney is the major site of BMP-7 expression during both embryogenesis and postnatal development (11). Pharmacological doses of BMP-7 can repair damaged renal tubules and preserve renal function in several models of renal diseases, including the Col4A3 knockout model of Alport syndrome (12–20). However, the exact role of endogenous BMP-7 and its mechanism of action remain unclear. In addition, the administration of recombinant BMP-7, whose target cells are widely expressed throughout the body, might also produce some undesired extrarenal effect.

The local activity of endogenous BMPs is controlled by certain classes of binding molecules that act as positive or negative regulators of BMP signaling activity (10, 21–24). BMP antagonists function through direct association with BMP, thus inhibiting the binding of BMP to its receptors and defining the boundaries of BMP activity.

The product of uterine sensitization–associated gene-1 (USAG-1) acts as a kidney-specific BMP antagonist, and USAG-1 binds to and inhibits the biological activity of BMP-7 (22, 25). USAG-1 is
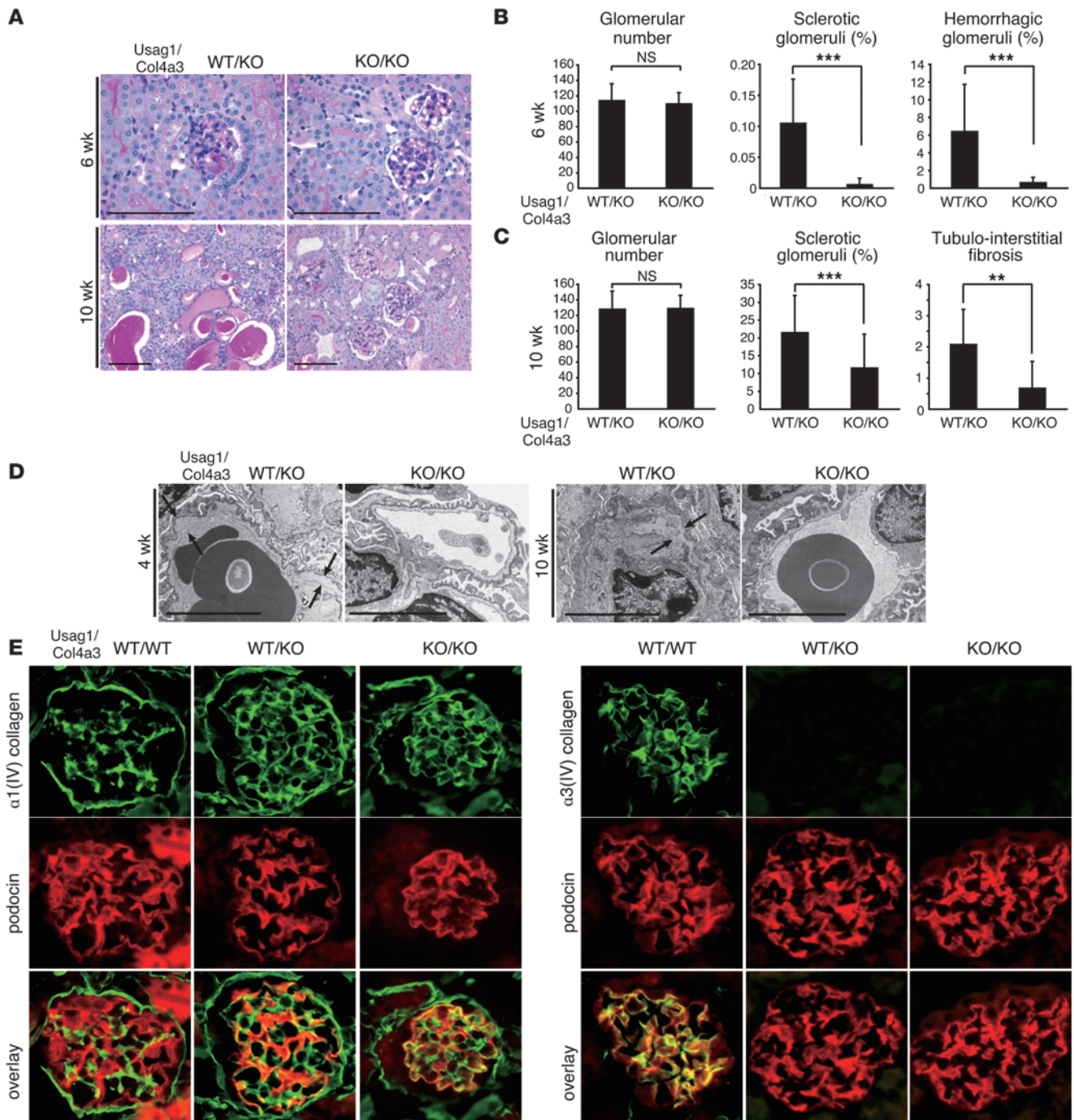
Figure 1
Usag1⁻/⁻Col4a3⁻/⁻ mice showed less glomerular and tubular injury. (**A**) Representative histological findings in *Usag1⁺/⁺Col4a3⁻/⁻* mice (WT/KO) and *Usag1⁻/⁻Col4a3⁻/⁻* mice (KO/KO) at 6 weeks and 10 weeks of age. Scale bars: 100 μm. (**B** and **C**) Quantitative assessment of the number of glomeruli, percentages of sclerotic and hemorrhagic glomeruli, and tubulointerstitial fibrosis score in *Usag1⁺/⁺Col4a3⁻/⁻* mice (WT/KO) and *Usag1⁻/⁻Col4a3⁻/⁻* mice (KO/KO) at 6 weeks (**B**, *n* = 5) and 10 weeks of age (**C**, *n* = 10). Bars indicate the mean ± SD. **$P < 0.01$; ***$P < 0.05$. (**D**) Electron microphotographs in *Usag1⁺/⁺Col4a3⁻/⁻* mice (WT/KO) and *Usag1⁻/⁻Col4a3⁻/⁻* mice (KO/KO) at 4 weeks and 10 weeks of age. Arrows indicate the splitting of GBM. Scale bars: 5 μm. (**E**) Immunostaining for α1(IV) and α3(IV) collagen in the glomeruli of WT littermates (WT/WT), *Usag1⁺/⁺Col4a3⁻/⁻* mice (WT/KO), and *Usag1⁻/⁻Col4a3⁻/⁻* mice (KO/KO) at 6 weeks of age. Podocin was used as a podocyte marker. Note the positive staining for α1(IV) collagen along with the GBM of *Usag1⁺/⁺Col4a3⁻/⁻* mice (WT/KO) and *Usag1⁻/⁻Col4a3⁻/⁻* mice (KO/KO), while the staining is restricted to mesangial areas in the glomeruli of WT littermates.
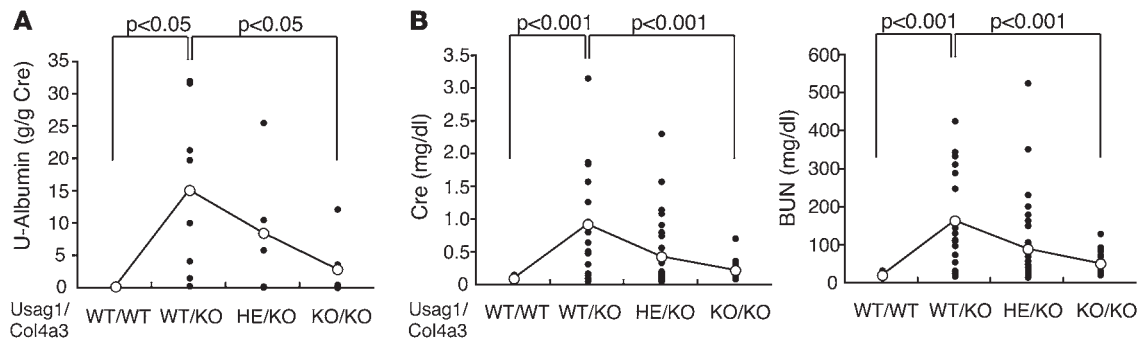
Figure 2
Usag1$^{-/-}$*Col4a3*$^{-/-}$ mice showed less albuminuria and preserved renal function. (**A**) Urinary albumin excretion normalized by urinary creatinine in WT littermates (WT/WT, n = 4), *Usag1*$^{+/+}$*Col4a3*$^{-/-}$ mice (WT/KO, n = 8), *Usag1*$^{+/-}$*Col4a3*$^{-/-}$ mice (HE/KO, n = 5), and *Usag1*$^{-/-}$*Col4a3*$^{-/-}$ mice (KO/KO, n = 7) at 6 weeks of age. Open circles represent mean value of each column, while closed circles represent individual mice. (**B**) Plasma creatinine and blood urea nitrogen (BUN) levels in WT littermates (WT/WT, n = 20), *Usag1*$^{+/+}$*Col4a3*$^{-/-}$ mice (WT/KO, n = 18), *Usag1*$^{+/-}$*Col4a3*$^{-/-}$ mice (HE/KO, n = 34), and *Usag1*$^{-/-}$*Col4a3*$^{-/-}$ mice (KO/KO, n = 17) at 10 weeks of age. Bars indicate mean ± SD. Open circles represent mean value of each column, while closed circles represent individual mice.

expressed in distal tubules and colocalizes with BMP-7 in distal convoluted tubules and connecting tubules (26). Furthermore, *Usag1*$^{-/-}$ mice are resistant to tubular injury such as acute renal failure and interstitial fibrosis, and USAG-1 is the central negative regulator of BMP function in the adult kidney (27). Because in adults the expression of USAG-1 is confined to the kidneys, targeting the activity of this protein might yield safer and more kidney-specific therapies than the administration of BMP-7 (23). For this, it will be important to first elucidate the role of USAG-1 in the pathology of progressive glomerular injury.

Here we show that genetic ablation of USAG-1 significantly attenuated the disease progression and preserved renal function in *Col4a3*$^{-/-}$ mice, a model for human Alport syndrome. The observations in this study suggest that USAG-1 might contribute to the pathogenesis of renal deterioration by a mechanism we believe to be novel that involves crosstalk between the macula densa of the distal tubules and the mesangium of the belonging glomerulus. In addition, we demonstrate that in the kidney of *Col4a3*$^{-/-}$ mice, TGF-β signaling includes phosphorylation of Smad1/5/8, transcription factors classically considered to be the downstream effectors of BMP signaling.

Results

Loss of USAG-1 slows progression of glomerular injury in Alport mice. *Col4a3*$^{-/-}$ mice, a mouse model of human Alport syndrome, develop progressive glomerulonephritis associated with tubulointerstitial fibrosis leading to renal failure. Kidneys from *Col4a3*$^{-/-}$ mice showed irregular thickening and splitting of the GBM at 4 weeks of age by electron microscopy. At 5 weeks of age, proteinuria is initiated, and at 6 weeks of age, minor glomerular lesion is occasionally observed by light microscopy. At 10 weeks of age, severe glomerular lesions associated with tubulointerstitial fibrosis are observed, and renal function deteriorates.

To test the role of USAG-1 in the progression of end-stage renal disease originating from glomerular injury, mice deficient in both *Col4a3* gene and *Usag1* gene were generated (*Usag1*$^{-/-}$*Col4a3*$^{-/-}$ mice). A histological examination of the kidneys from *Usag1*$^{+/+}$*Col4a3*$^{-/-}$ mice revealed segmental sclerosis and intraglomerular hemorrhage at 6 weeks of age, while these changes were almost completely absent in *Usag1*$^{-/-}$*Col4a3*$^{-/-}$ mice (Figure 1, A and B). At 10 weeks of age, *Usag1*$^{+/+}$*Col4a3*$^{-/-}$ mice demonstrated glomerulosclerosis associ-

ated with inflammatory cell infiltration, interstitial fibrosis, tubular atrophy, and cast formation, while these changes significantly decreased in *Usag1*$^{-/-}$*Col4a3*$^{-/-}$ mice (Figure 1, A and C).

An ultrastructural analysis of GBM using transmission electron microscopy at 4 weeks of age showed that *Usag1*$^{+/+}$*Col4a3*$^{-/-}$ mice had extensive splitting of the GBM, while *Usag1*$^{-/-}$*Col4a3*$^{-/-}$ mice showed almost normal GBM structure (Figure 1D). *Usag1*$^{-/-}$*Col4a3*$^{-/-}$ mice at 10 weeks of age also exhibited a significant preservation of GBM structure in comparison with age-matched *Usag1*$^{+/+}$*Col4a3*$^{-/-}$ mice (Figure 1D).

The immunostaining of α1(IV) or α3(IV) collagen was performed to compare the glomerular localization of α(IV) collagen in both genotypes (Figure 1E). The expression of α1(IV) collagen was detected in the GBM of both *Usag1*$^{+/+}$*Col4a3*$^{-/-}$ and *Usag1*$^{-/-}$*Col4a3*$^{-/-}$ mice, while the expression was confined to mesangial area in the WT mice. The expression of α3(IV) collagen was absent in the GBM of both *Usag1*$^{+/+}$*Col4a3*$^{-/-}$ and *Usag1*$^{-/-}$*Col4a3*$^{-/-}$ mice, while the expression was detected along the GBM in the WT mice. Therefore, regardless of the presence or absence of USAG-1, no alteration was observed in the glomerular localization of α(IV) collagen.

Usag1$^{-/-}$*Col4a3*$^{-/-}$ *mice showed less albuminuria, preserved renal function, and longer life span.* An analysis of urinary albumin excretion at 6 weeks of age is shown in Figure 2A, demonstrating significantly less albuminuria in *Usag1*$^{-/-}$*Col4a3*$^{-/-}$ mice than in *Usag1*$^{+/+}$*Col4a3*$^{-/-}$ mice. The systolic blood pressure of *Usag1*$^{-/-}$*Col4a3*$^{-/-}$ mice at 5 weeks of age was slightly lower than that of *Usag1*$^{+/+}$*Col4a3*$^{-/-}$ mice (Supplemental Figure 2; supplemental material available online with this article; doi:10.1172/JCI39569DS1). Renal function of *Usag1*$^{-/-}$*Col4a3*$^{-/-}$ mice at 10 weeks of age, as assessed by serum creatinine and blood urea nitrogen, was also significantly preserved in comparison with that of *Usag1*$^{+/+}$*Col4a3*$^{-/-}$ mice (Figure 2B), consistent with the results of renal histology and urinary albumin excretion. Furthermore, upon aging beyond 13 weeks, *Usag1*$^{-/-}$*Col4a3*$^{-/-}$ mice showed less mortality than *Usag1*$^{+/+}$*Col4a3*$^{-/-}$ mice (Supplemental Figure 1).

Inflammatory cytokine expression was significantly reduced in Usag1$^{-/-}$*Col4a3*$^{-/-}$ *mice.* As previously reported, the mRNA of inflammatory cytokines such as TNF-α, IL-1β, monocyte chemoattractant protein-1 (MCP-1), and TGF-β was upregulated in the kidneys of *Usag1*$^{+/+}$*Col4a3*$^{-/-}$ mice at 10 weeks of age (28, 29). In *Usag1*$^{-/-}$*Col4a3*$^{-/-}$ mice, however, increases in inflammatory cytokines were signifi-
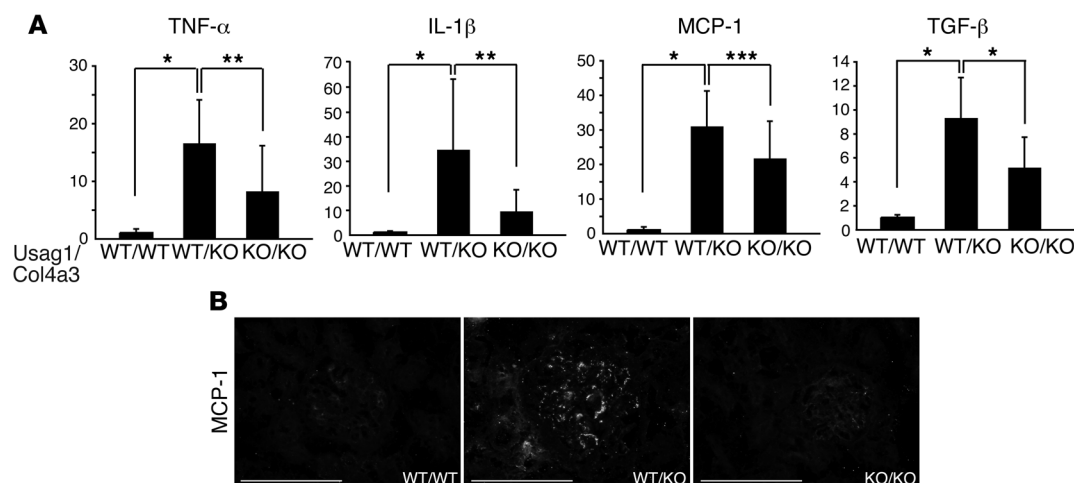
Figure 3
The expression of inflammatory cytokines significantly decreased in the kidneys of $Usag1^{-/-}Col4a3^{-/-}$ mice. (**A**) Real-time RT-PCR analysis of inflammatory cytokine mRNA in the kidneys of WT littermates (WT/WT), $Usag1^{+/+}Col4a3^{-/-}$ mice (WT/KO), and $Usag1^{-/-}Col4a3^{-/-}$ mice (KO/KO) at 10 weeks of age. The expression levels were normalized to those of GAPDH and expressed relative to those of WT littermates ($n = 10$). Bars indicate the mean ± SD. *$P < 0.001$; **$P < 0.01$; ***$P < 0.05$. (**B**) Representative immunostaining for MCP-1 in the kidneys of WT littermates (WT/WT), $Usag1^{+/+}Col4a3^{-/-}$ mice (WT/KO), and $Usag1^{-/-}Col4a3^{-/-}$ mice (KO/KO) at 10 weeks of age. Scale bars: 100 μm.

cantly attenuated (Figure 3A). Immunostaining for MCP-1 revealed faint expression of MCP-1 in the glomeruli of $Usag1^{-/-}Col4a3^{-/-}$ mice in comparison with $Usag1^{+/+}Col4a3^{-/-}$ mice (Figure 3B).
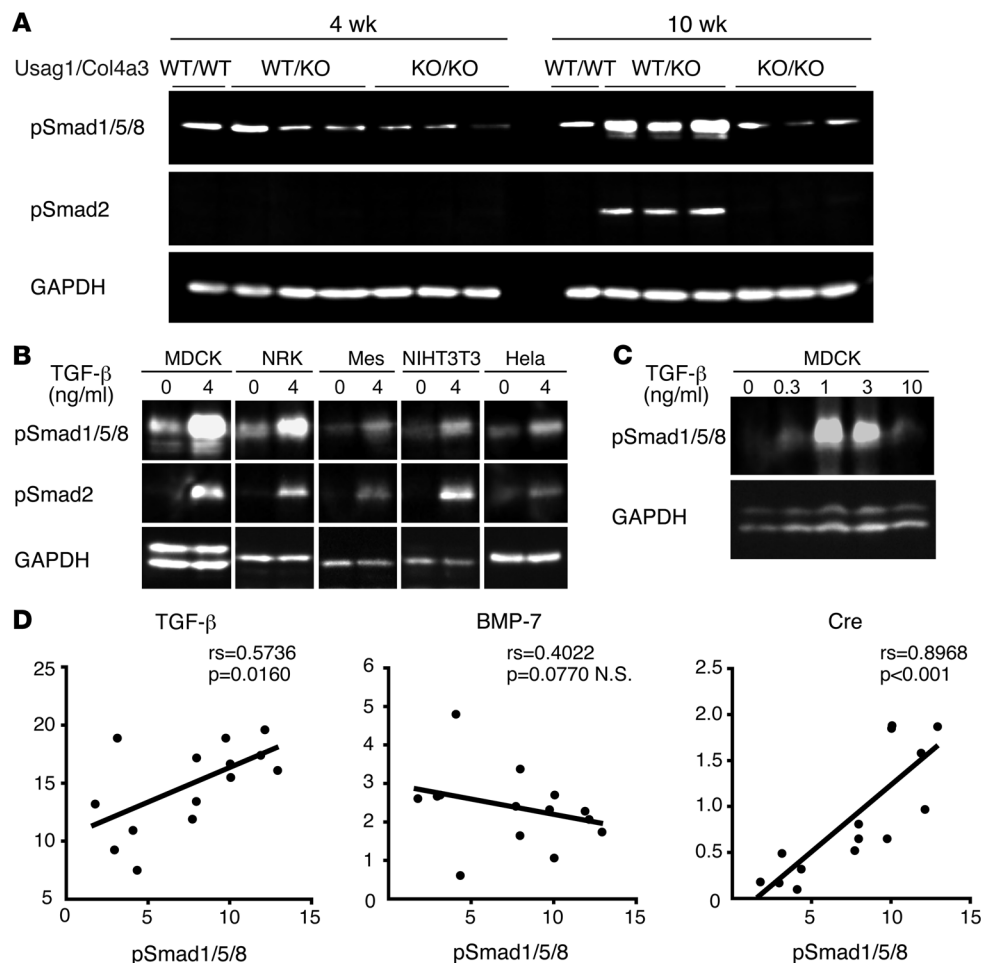
Enhanced Smad1/5/8 phosphorylation in $Usag1^{+/+}Col4a3^{-/-}$ mice, but not in $Usag1^{-/-}Col4a3^{-/-}$ mice, was possibly activated by TGF-β signaling. Next, the activation of Smad signaling was examined. The traditional view of the TGF-β superfamily signaling pathways assumes 2 distinct branches: a TGF-β branch that signals through Smad2/3 and a BMP branch that signals through Smad1/5/8 (30).

We observed increased phosphorylation of Smad2, the TGF-β signal transducer, in the kidneys of $Usag1^{+/+}Col4a3^{-/-}$ mice as compared with WT mice as well as $Usag1^{-/-}Col4a3^{-/-}$ mice (Figure 4A), consistent with high expression of TGF-β in $Usag1^{+/+}Col4a3^{-/-}$ mice (Figure 3A). The phosphorylation of Smad1/5/8, the classical BMP signal transducer, was expected to be reduced in the kidneys of $Usag1^{+/+}Col4a3^{-/-}$ mice due to generally low expression of BMP-7 in kidney disease models (12, 17, 26, 31). However, the phosphorylation of Smad1/5/8 was unexpectedly increased in the kidneys of $Usag1^{+/+}Col4a3^{-/-}$ mice in comparison with WT mice as well as $Usag1^{-/-}Col4a3^{-/-}$ mice.

Recently, several groups demonstrated that TGF-β activates Smad1/5 in addition to Smad2/3 in endothelial cells through novel receptor complexes (32–34). Thus, we hypothesized that the increased phosphorylation of Smad1/5/8 in the kidneys of $Usag1^{+/+}Col4a3^{-/-}$ mice might also have resulted from high expression of TGF-β. To test this hypothesis, we administered TGF-β to various types of cells including MDCK cells, primary mesangial cells, NRK cells (rat tubule epithelial cells), NIH3T3 cells, and HeLa cells, and demonstrated that TGF-β can activate the phosphorylation of Smad1/5/8 in addition to Smad2 in all these cell types (Figure 4B). The phosphorylation of Smad1/5/8 was induced by TGF-β at concentrations as low as 1 ng/ml (Figure 4C). Furthermore, the phosphorylation of Smad1/5/8 in the kidneys of $Usag1^{+/+}Col4a3^{-/-}$ mice correlated well with renal TGF-β as well as with serum creatinine levels, but not with the expression of BMP-7 (Figure 4D). Taken together, these results indicate that enhanced phosphorylation of Smad1/5/8 in

$Col4a3^{-/-}$ mice might be due to TGF-β signaling and attenuated phosphorylation of Smad1/5/8 in $Usag1^{-/-}Col4a3^{-/-}$ mice might reflect reduced expression of TGF-β and disease severity.

$Usag1^{-/-}Col4a3^{-/-}$ mice showed less expression and activity of MMPs in the kidneys. Previous reports have demonstrated the important roles of MMPs in increasing susceptibility of defective Alport GBM to proteolytic degradation (9). The expression of *MMP* mRNA reported to be involved in this model was analyzed in the kidneys of 10-week-old mice, and this demonstrated strong upregulation of MMP-2, MMP-3, MMP-7, MMP-9, and MMP-12 in the kidneys of $Usag1^{+/+}Col4a3^{-/-}$ mice, while the expression of these MMPs was significantly less increased in the kidneys of $Usag1^{-/-}Col4a3^{-/-}$ mice (Figure 5A). The proteolytic activity of these MMPs in the kidney extracts was also determined by casein and gelatin zymography. Casein zymography showed a significant reduction in MMP-7 and MMP-12 activities (Figure 5B), and gelatin zymography demonstrated significant reduction of MMP-2 activity in the kidneys of $Usag1^{-/-}Col4a3^{-/-}$ mice in comparison with $Usag1^{+/+}Col4a3^{-/-}$ mice (Figure 5C). Also, the bands seen at 57 and 45 kDa in gelatin zymography, possibly representing MMP-3 activity (35), were significantly less in the kidneys of $Usag1^{-/-}Col4a3^{-/-}$ mice. Recently, it was demonstrated that expression of MMP-12 was markedly upregulated in the glomeruli of $Usag1^{+/+}Col4a3^{-/-}$ mice, and inhibition of MMP-12 preserved the integrity of GBM (29). Immunostaining for MMP-12 demonstrated a significant upregulation in the glomeruli and interstitium of $Usag1^{+/+}Col4a3^{-/-}$ mice, while the induction was attenuated in $Usag1^{-/-}Col4a3^{-/-}$ mice (Figure 5D). While MMP-12 is expressed by macrophages as well as glomerular cells such as podocytes (29, 36, 37), immunostaining of CD11b, a marker of monocytes and tissue macrophages, failed to demonstrate any significant infiltration of macrophages or monocytes in the glomeruli of 10-week-old $Usag1^{+/+}Col4a3^{-/-}$ mice (data not shown), suggesting that the glomerular MMP-12 in Alport mice was not due to the macrophages that infiltrated the glomeruli.

Figure 4
Smad1/5/8 phosphorylation was enhanced in $Usag1^{+/+}Col4a3^{-/-}$ mice, but not in $Usag1^{-/-}Col4a3^{-/-}$ mice. (**A**) Representative immunoblotting for Smad phosphorylation in the kidneys of WT littermates (WT/WT), $Usag1^{+/+}Col4a3^{-/-}$ mice (WT/KO), and $Usag1^{-/-}Col4a3^{-/-}$ mice (KO/KO) at 4 and 10 weeks of ages. (**B**) A panel of cell lines were tested for the ability of TGF-β to induce phosphorylation of Smad1/5/8 in addition to Smad2. Cells were either left untreated or stimulated with 4 ng/ml of TGF-β for 1 hour. Whole-cell extracts were analyzed by immunoblotting using antibodies against phosphorylated Smad1/5/8 (pSmad1/5/8), pSmad2, and GAPDH as a loading control. (**C**) Representative immunoblotting showing the effect of various concentrations of TGF-β on the phosphorylation of Smad1/5/8 in MDCK cells. (**D**) Correlation between the phosphorylation levels of Smad1/5/8 in the kidneys of $Usag1^{+/+}Col4a3^{-/-}$ mice and mRNA expression of TGF-β and BMP-7 and serum creatinine ($n = 14$). The levels of phosphorylation of Smad1/5/8 were determined using the LAS image analysis system.

USAG-1 was not expressed in the Alport glomeruli. USAG-1 is expressed predominantly in the distal tubules, more specifically, in the thick ascending limb, distal convoluted tubules, and connecting tubules in adult kidneys, and not expressed in glomeruli (26). In situ hybridization was used to determine the expression of USAG-1 in $Usag1^{+/+}Col4a3^{-/-}$ mice and demonstrated that USAG-1 expression was not detectable in the glomeruli of $Usag1^{+/+}Col4a3^{-/-}$ mice either (Figure 6A) and was confined to tubules.

USAG-1 colocalizes with BMP-7 in the macula densa. Deficiency of USAG-1 significantly attenuated glomerular pathology in the $Col4a3^{-/-}$ mouse model of Alport syndrome in spite of the absence of USAG-1 expression in glomeruli. Further experiments focused on the part of the distal tubule that came in contact with its own glomerulus, the macula densa (Figure 6B). To determine whether USAG-1 is expressed in macula densa cells, we performed double staining of nNOS, a specific marker for macula densa, and β-gal using $Usag1^{+/LacZ}$ mice. As shown in Figure 6C, β-gal staining as well as immunostaining with anti-LacZ antibody colocalized with nNOS staining, indicating that USAG-1 was expressed in macula densa. BMP-7 is expressed in distal convoluted tubules, connecting tubules, collecting ducts, and podocytes (26). β-gal staining as well as immunostaining with anti-LacZ antibody also colocalized with nNOS in the kidneys of $Bmp7^{+/LacZ}$ mice, indicating the expression of BMP-7 in the macula densa (Figure 6C). Therefore, USAG-1 colocalizes with BMP-7 in the macula densa cells.

BMP-7 suppressed TGF-β–induced MMP-12 upregulation in mesangial cells, and USAG-1 antagonized the action of BMP-7. The macula densa, in which both USAG-1 and BMP-7 are expressed, is adjacent to mesangial cells in its own glomerulus (Figure 6B). To investigate potential mechanisms that are responsible for the beneficial effect of USAG-1 deficiency in Alport syndrome, the effect of BMP-7 and USAG-1 in cultured mesangial cells was examined. The expression of MMP-12 in cultured mesangial cells was upregulated by the administration of IL-1β and TGF-β, but not by the administration of MCP-1 (Figure 6D), in spite of the fact that MCP-1 is reported to stimulate MMP-12 expression in podocytes (29). The administration of BMP-7 suppressed TGF-β–induced MMP-12 upregulation in mesangial cells, and simultaneous administration of USAG-1 antagonized the suppressive effect of BMP-7 (Figure 6E). These results indicate that USAG-1 might enhance MMP-12 expression in the glomeruli by suppressing the inhibitory effect of BMP-7 and exacerbate glomerular disease progression in Alport syndrome.

Discussion

This study demonstrates that USAG-1 accelerates glomerular pathogenesis in a mouse model of human Alport syndrome, possibly through the crosstalk between the kidney tubules and its own glomerulus. $Usag1^{-/-}Col4a3^{-/-}$ mice demonstrated attenuated glomerular disease progression and preserved renal function in comparison with $Usag1^{+/+}Col4a3^{-/-}$ mice and significantly decreased
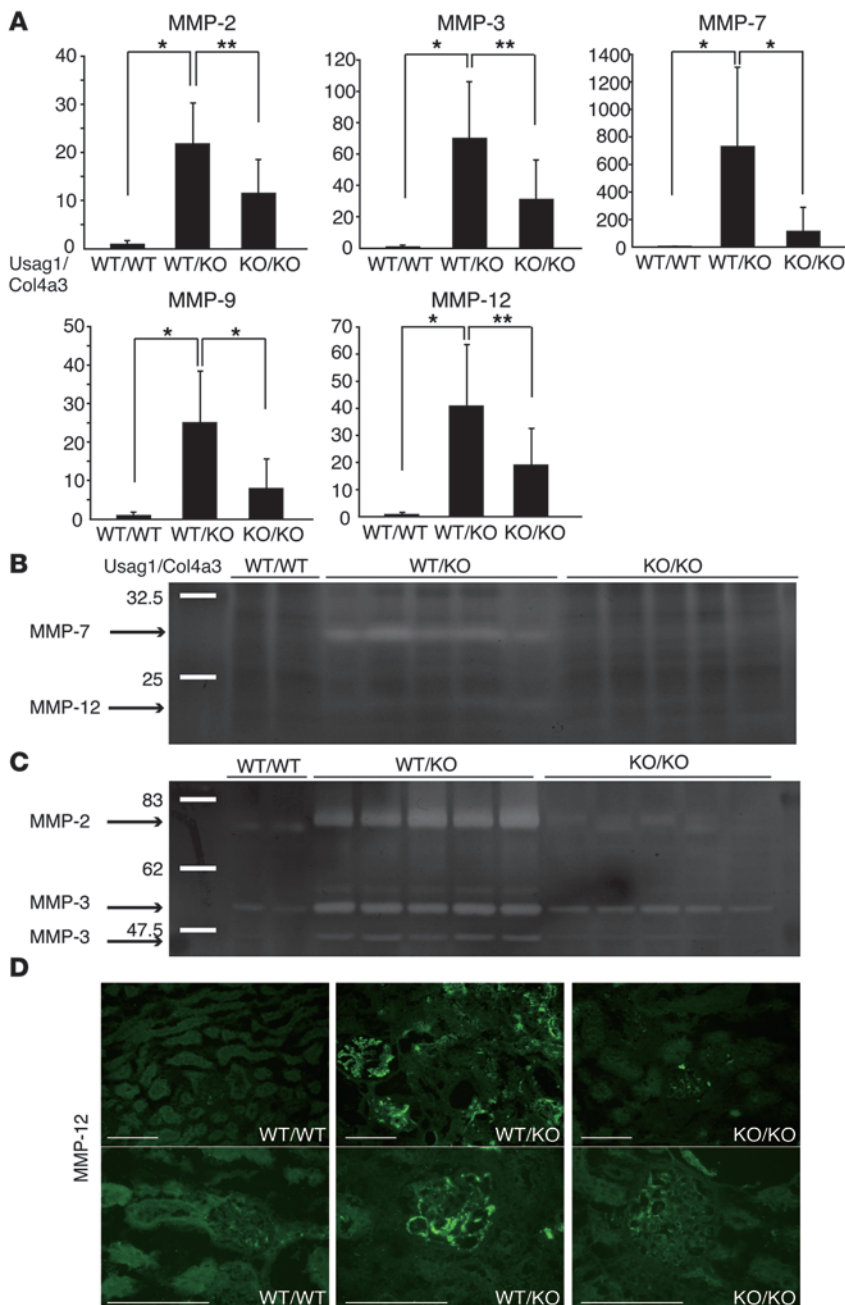
Figure 5
Usag1⁻/⁻Col4a3⁻/⁻ mice showed less expression and activity of MMPs in the kidneys. (**A**) Real-time RT-PCR analysis of MMP mRNA in the kidneys of WT littermates (WT/WT), *Usag1⁺/⁺Col4a3⁻/⁻* mice, (WT/KO) and *Usag1⁻/⁻Col4a3⁻/⁻* mice (KO/KO) at 10 weeks of age. The expression levels were normalized to that of GAPDH and expressed relative to that in WT littermates (*n* = 10). Bars indicate the mean ± SD. *P < 0.001; **P < 0.01. (**B**) Casein zymography analyzing the kidneys of WT littermates (WT/WT), *Usag1⁺/⁺Col4a3⁻/⁻* mice (WT/KO), and *Usag1⁻/⁻Col4a3⁻/⁻* mice (KO/KO) at 10 weeks of age. (**C**) Gelatin zymography analyzing the kidneys of WT littermates (WT/WT), *Usag1⁺/⁺Col4a3⁻/⁻* mice (WT/KO), and *Usag1⁻/⁻Col4a3⁻/⁻* mice (KO/KO) at 10 weeks of age. (**D**) Representative immunostaining for MMP-12 in the kidneys of WT littermates (WT/WT), *Usag1⁺/⁺Col4a3⁻/⁻* mice (WT/KO), and *Usag1⁻/⁻Col4a3⁻/⁻* mice (KO/KO) at 10 weeks of age. Scale bars: 100 μm.

expression and activity of MMPs, which play key roles in disease progression of Alport syndrome. Furthermore, USAG-1 and BMP-7 colocalized in the macula densa, a part of the distal tubules in contact with its own glomerulus, and BMP-7 reduced MMP-12 expression in mesangial cells, which was antagonized by USAG-1.

USAG-1 exacerbates glomerular injuries as well as tubular interstitial fibrosis. Tubular damage and interstitial fibrosis are the final common pathways leading to end-stage renal disease (ESRD) (38, 39) irrespective of the nature of the initial renal injury, and the degree of tubular damage parallels the impairment of renal function (39). Severe tubulointerstitial fibrosis is observed following glomerular injury in *Col4a3⁻/⁻* mice, and this exacerbates renal function. Because *Usag1⁻/⁻* mice were resistant to tubulointerstitial fibrosis

(27), this resistance might contribute at least in part to the preservation of renal function in *Usag1⁻/⁻Col4a3⁻/⁻* mice. In addition, *Usag1⁻/⁻Col4a3⁻/⁻* mice showed preserved GBM with less albuminuria in the early stage when tubular injury has yet to appear. Therefore, *Usag1⁻/⁻Col4a3⁻/⁻* mice were resistant to both glomerular and tubular injuries.
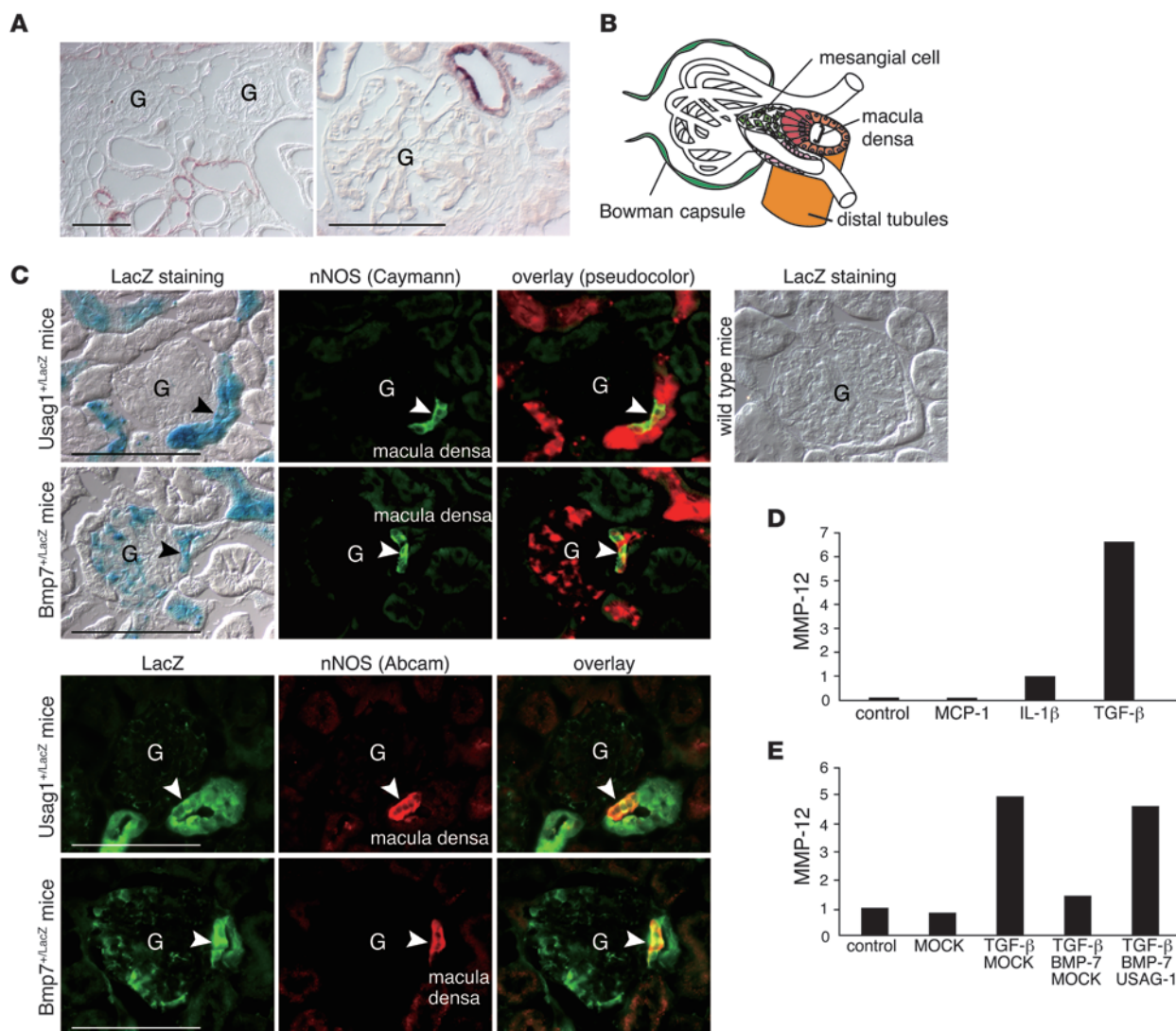
USAG-1 increases the expression of MMP in Col4a3⁻/⁻ mice. The molecular mechanisms by which the altered GBM composition in Alport syndrome causes renal pathogenesis remain unclear. It is proposed that abnormal persistence of α1/α1/α2(IV) collagen network in the adult GBM is associated with increased susceptibility to proteolysis by proteases in Alport syndrome (3, 9) and pharmacological ablation of MMP activities, especially MMP-12, leads to a significant attenuation in Alport disease progression (29, 40). The expression and activities of MMPs were significantly upregulated in the kidneys of *Usag1⁺/⁺Col4a3⁻/⁻* mice, which is consistent with previous reports, and they were suppressed in the kidneys of *Usag1⁻/⁻Col4a3⁻/⁻* mice. The suppression of MMP activities probably contributed, at least in part, to slow glomerular pathogenesis in *Usag1⁻/⁻Col4a3⁻/⁻* mice. In addition, the administration of BMP-7 decreased the expression of MMP-12 in cultured mesangial cells, and USAG-1 antagonized the action of BMP-7. Therefore, USAG-1 might increase the expression of MMP in glomeruli and accelerate GBM destruction in *Col4a3⁻/⁻* mice.

Other possible roles of USAG-1 and BMP-7 in glomerular pathogenesis in Col4a3⁻/⁻ mice. In addition to the inhibitory effect on MMP expression, BMP-7 possibly inhibits the progression of glomerular pathogenesis in *Col4a3⁻/⁻* mice at multiple steps. BMP-7 reduces the damage in podocytes (20, 41, 42) and mesangial cells (43–45) and attenuates the expression of inflammatory cytokines (46) and
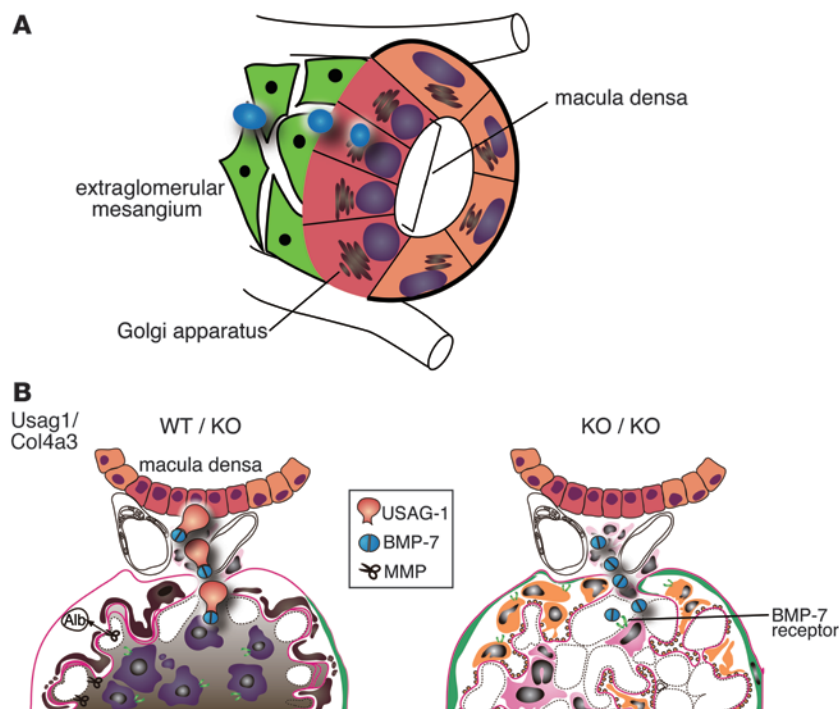
Figure 6
USAG-1 colocalizes with BMP-7 in the macula densa and inhibits the action of BMP-7 in mesangial cells. (**A**) In situ hybridization for USAG-1 mRNA in the kidneys of 10-week-old *Col4a3*−/− mice. Scale bars: 100 μm. G, glomerulus. (**B**) A schematic illustration of the juxtaglomerular apparatus. The macula densa is a part of distal tubules contacting with its glomerulus of origin and adjacent to mesangial cells. (**C**) β-Gal staining as well as immunostaining with anti-LacZ antibody colocalized with immunostaining with anti-nNOS (a marker for macula densa) antibody in the kidneys of *Usag1*+/*LacZ* mice and *Bmp7*+/*LacZ* mice. Kidney section from WT mice was also treated in the same way with the sections from *Usag1*+/*LacZ* mice and *Bmp7*+/*LacZ* mice and demonstrated no β-gal staining. Scale bars: 100 μm. (**D**) Real-time RT-PCR analysis of MMP-12 mRNA in cultured mesangial cells treated with inflammatory cytokines. The expression levels were normalized to those of GAPDH and expressed relative to those in controls. TGF-β markedly increased MMP-12 mRNA expression in mesangial cells. The graph reflects data that are representative for results of 4 independent experiments. (**E**) Real-time RT-PCR analysis of MMP-12 mRNA in cultured mesangial cells that were incubated with TGF-β, BMP-7, and USAG-1. BMP-7 suppressed TGF-β–induced MMP-12 upregulation in mesangial cells, and USAG-1 reversed the action of BMP-7. The graph reflects data that are representative for results of 4 independent experiments.

apoptosis in several types of cells (12, 41). Antagonizing the beneficial effects of BMP-7 by USAG-1 might enhance these injuries and accelerate glomerular pathogenesis in Alport syndrome.

USAG-1 secreted from distal tubules reaches the glomerulus and accelerates glomerular injury. Although the mechanism by which USAG-1 secreted from distal tubules reaches the glomerulus and exacerbates glomerular pathogenesis is not entirely clear, a crosstalk may exist between the distal tubule and the glomerulus in the same nephron.

The distal tubule of a nephron makes contact with the vascular pole of its glomerulus from which the distal tubule originated. At this point, there is a plaque of very specialized and differentiated cells in the distal tubule known as the macula densa (Figure 6B). The macula densa detects changes in the distal tubular fluid composition and transmits signals to the adjacent extraglomerular mesangial cells and afferent arterioles (47–53). Extraglomerular mesangial cells are anatomically in continuity with the glomerular mesangial cells and transmit the signal from the macula densa to the glomeru-

Figure 7
Hypothetical model for involvement of USAG-1 secreted from distal tubules in the pathogenesis of glomerular damage in Alport syndrome. (**A**) The macula densa (red), a part of the distal tubules, lies beside the extraglomerular mesangial cells (green), and the nuclei of the macula densa cells are apically located, suggesting the possibility that substances (blue) might be secreted from the basolateral membrane of the macula densa. Note that the basement membrane of the macula densa cells is continuous with the basement membrane of the extraglomerular mesangial cells. (**B**) In *Usag1*^{+/+}*Col4a3*^{−/−} mice (WT/KO), the mesangial cells are activated (purple) and secrete MMPs (scissors), which degrade GBM. Following GBM destruction, podocytes residing on the GBM are damaged (brown) and albuminuria is observed. BMP-7 (blue) secreted from the macula densa is captured by USAG-1, which is also secreted from the macula densa. As a consequence, BMP-7 cannot bind to its receptors and exert its renoprotective action. In *Usag1*^{−/−}*Col4a3*^{−/−} mice (KO/KO), BMP-7 secreted from the macula densa can bind to its receptors on mesangial cells and podocytes, and protect fragile alport GBM from degradation.

lus. The signals from the macula densa to the mesangial cells involve small diffusible substances (ATP or adenosine) released from the macula densa (47, 54). Multiphoton imaging demonstrates the water flow across the macula densa into the mesangial cell field at varying osmolarities in the luminal fluid (47). The histological characteristics of the macula densa also support the idea of substance transportation from the macula densa to mesangial cells: the nuclei of macula densa cells are apically located, while most of cell organelles tend to be located basally and laterally, thus indicating that the substances from the macula densa are possibly secreted basolaterally (Figure 7A). In addition, the basement membrane of the macula densa is fused with the basement membrane of the extraglomerular mesangial cells, indicating the lack of a barrier to interfere with substance transportation from the macula densa to the glomerulus (Figure 7A). Furthermore, Hugo et al. demonstrated that extraglomerular mesangial cells function as reserve cells for glomerular mesangial cells (55). Extraglomerular mesangial cells stimulated by substances secreted from the macula densa migrate into glomerulus after glomerular injury and repopulate as mesangial cells.

As shown in Figure 6C, both USAG-1 and BMP-7 are expressed in the macula densa, and USAG-1 secreted from the basolateral membrane of macula densa could inhibit the action of BMP-7 on the adjacent mesangial cells. In the experiments using cultured mesangial cells, BMP-7 significantly attenuated TGF-β–induced MMP-12 upregulation, and the inhibitory effect of BMP-7 was abolished by the addition of USAG-1. Moreover, BMP-7 reduced TGF-β–induced cytotoxicity in mesangial cells (data not shown). Therefore, USAG-1 might exacerbate glomerular pathogenesis in Alport syndrome through accelerating upregulation of GBM-degrading enzyme and cytotoxicity by inhibiting the reno-protective effects of BMP-7 (Figure 7B).

An alternative possibility that may explain the effect of USAG-1 on glomerular injury is an interaction between circulating USAG-1 and BMP-7 in plasma. BMP-7 is present in plasma at a concentra-

tion range of 100–300 pg/ml (12). Due to the lack of an effective ELISA system, the plasma level of USAG-1 remains to be determined. If an appropriate amount of USAG-1 is present in the circulation, it could therefore bind to BMP-7 and thus inhibit its activity. To test the effect of circulating USAG-1 in the progression of *Col4a3*^{−/−} mice, we performed systemic gene transfer of USAG-1 expression vector to *Usag1*^{−/−}*Col4a3*^{−/−} mice and demonstrated that the difference in albuminuria between the gene transfer group and the control group was not statistically significant (Supplemental Figure 3).

Novel therapeutic approach for Alport syndrome. At present there is no definitive therapy to prevent or slow renal disease progression in Alport syndrome. Several studies using a mouse model of Alport syndrome have provided potential therapies, such as MMP inhibitor (29, 40), angiotensin-converting enzyme inhibitor (56), statins (57), transplantation of bone marrow–derived stem cells (58–60), and total body irradiation (61). The results of the present study support the notion that therapeutic trials to inhibit the function of USAG-1 may become a novel therapeutic approach for Alport syndrome either alone or in combination with other approaches. A therapeutic trial targeting USAG-1 is promising because it is expected to be effective in both glomerular and tubular injuries, is more kidney-specific, and has fewer extrarenal effects because the expression of USAG-1 is confined to the kidney.

Methods

Mice. The *Usag1*^{−/−} mice used in this study have been described previously (27), and *Col4a3*^{−/−} mice were purchased from Jackson Laboratory (JAX mice strain 129-Col4a3[tm1Dec]/J) (62). *Usag1*^{−/−}*Col4a3*^{−/−} mice were generated by breeding *Usag1*^{+/−} and *Col4a3*^{+/−} mice. *Col4a3*^{−/−} littermates (*Usag1*^{+/+}*Col4a3*^{−/−} mice) and WT littermates (*Usag1*^{+/+}*Col4a3*^{+/+} mice) served as controls. All animal studies were approved by the Animal Research Committee, Graduate School of Medicine, Kyoto University, and performed in accordance with the guidelines of Kyoto University.

Age-matched mice were used for all studies. The ages of mice used in each experiment are described below.

Assessment of albuminuria. The mice were placed in metabolic cages, and urine was collected over a 24-hour period. During the urine collection, mice were allowed free access to food and water. Urinary albumin concentration was measured using the Albuwell M assay kit (Exocell).

Renal histopathology and electron microscopy. The kidneys were fixed in Carnoy's solution and embedded in paraffin. Sections (2-μm thick) were stained with PAS for routine histological examination, and the degree of morphological change was determined for ten 10-week-old mice and five 6-week-old mice per group by experienced pathologists who were blinded to the genotypes. The following parameters were evaluated: percentage of hemorrhagic glomeruli and sclerotic glomeruli; and tubular atrophy/interstitial fibrosis score. Tubular atrophy/interstitial fibrosis was graded as follows: grade 0, 0%–24%; grade 1, 25%–49%; grade 2, 50%–74%; grade 3, ≥ 75%.

Frozen sections of the kidneys were immunostained as previously described (63). The primary antibodies were against podocin (64), α1 (H11), and α3 (H31) chains of type IV collagen (a gift from Y. Sado; ref. 65), MCP-1 (R&D Systems), MMP-12 (Santa Cruz Biotechnology Inc.), nNOS (Cayman Chemical and Abcam), and LacZ (Cappel Laboratory). For double staining with β-gal, immunostaining was performed before β-gal staining to avoid the possibility that the deposition of X-gal might interfere with the antibody binding to the antigen. For electron microscopy, portions of the cortex were fixed in 2% glutaraldehyde and post-fixed in 1% osmic acid. After embedding, ultrathin sections were stained with uranyl acetate and lead citrate.

β-Gal staining and in situ hybridization. β-Gal staining and in situ hybridization were performed as described previously (26, 66). The probe for in situ hybridization of *USAG-1* mRNA contained the 1.0-kb open reading frame with GC content of 52.6%. Hybridization was detected using an anti-digoxigenin antibody conjugated with alkaline phosphatase and Nitro blue tetrazolium chloride/5-bromo-4-chloro-3-indolyl phosphate, 4-toluidine salt (Roche Diagnostics).

Immunoblotting. Whole-kidney tissue was homogenized in RIPA buffer and subjected to immunoblotting as previously described (67). The primary antibodies were anti–phospho-Smad1/5/8 (Cell Signaling Technology), phospho-Smad2 (Upstate Biotechnology), and GAPDH (Fitzgerald Industries).

Quantification of mRNA by real-time RT-PCR. Real-time RT-PCR was performed as described previously (27). Specific primers were designed using Primer Express software (Applied Biosystems). Serially diluted cDNA was used to generate the standard curve for each primer, and the PCR conditions were as follows: 50°C for 2 minutes, 95°C for 10 minutes, then 95°C for 15 seconds, and 60°C for 1 minute for 40 cycles.

Cell cultures. Mouse mesangial cells were established from glomeruli isolated from a 4-week-old normal mouse (C57BL/6J) and characterized as described previously (68). Cells of passage numbers 18 to 21 were cultured in DMEM/F12 containing 20% fetal calf serum.

Assessment of MMP mRNA expression in mesangial cells. Mesangial cells were seeded at a concentration of 5×10^4/ml. After 24 hours, the culture medium was replaced with DMEM containing 0.5% bovine serum albumin. The cells were incubated for 72 hours with 10 ng/ml MCP-1 (R&D Systems), 250 pg/ml IL-1β (R&D Systems), or 3 ng/ml TGF-β (R&D Systems) in the presence or absence of 20 ng/ml BMP-7 (R&D Systems) and then were analyzed for *MMP* mRNA expression by real-time RT-PCR. All experiments were performed in quadruplicate.

Production of recombinant USAG-1–Flag protein. A recombinant C-terminally Flag-tagged USAG-1 protein (USAG-1–Flag) was produced using the Baculovirus Expression System (Invitrogen) and purified from culture medium by affinity absorption on anti-FLAG M2 affinity beads (Sigma-Aldrich). Protein concentrations were estimated by Coomassie staining.

Zymography. Renal proteins were extracted as previously described (69). Samples standardized for protein concentration of 60 μg/lane were electrophoretically separated in 10% SDS-polyacrylamide gels that contained 1 mg/ml gelatin or α-casein. After separation, gels were placed in 2.5% Triton X-100 in PBS, washed, and incubated in developing buffer (50 mM Tris, pH 7.5, 200 mM NaCl, 5 mM CaCl2, and 0.02% Brij-35) overnight at 37°C. The gels were stained with 0.5% Coomassie blue R250 and then destained with a 10% acetic acid, 40% methanol solution until the gelatinolytic bands were clearly seen.

Systemic gene transfer. Usag1$^{-/-}$Col4a3$^{-/-}$ mice were injected with 300 μg of pcDNA3.1mUSAG-1 (cDNA for mouse USAG-1 cloned into the pcDNA3.1 expression vector) into the tibialis anterior muscle at 6 weeks as described (70) and were analyzed at 8 weeks for urinary albumin and renal histology.

Statistics. Data are presented as the mean ± SD. Statistical significance was assessed by Student's *t* test for 2 group comparisons and by ANOVA, followed by Fisher's protected least significant difference post-hoc test for multiple group comparisons. Significance was defined as a value of $P < 0.05$.

Address correspondence to: Motoko Yanagita, Career-Path Promotion Unit for Young Life Scientists, Kyoto University Graduate School of Medicine, Yoshida-konoe-cho, Sakyo-ku, Kyoto 606-8501, Japan. Phone: 81.75.753.9310; Fax: 81.75.753.9311; E-mail: motoy@kuhp.kyoto-u.ac.jp.

1. Kalluri R. Basement membranes: structure, assembly and role in tumour angiogenesis. *Nat Rev Cancer.* 2003;3(6):422–433.
2. Timpl R. Structure and biological activity of basement membrane proteins. *Eur J Biochem.* 1989;180(3):487–502.
3. Hudson BG, Tryggvason K, Sundaramoorthy M, Neilson EG. Alport's syndrome, Goodpasture's syndrome, and type IV collagen. *N Engl J Med.* 2003;348(25):2543–2556.
4. Pescucci C, Longo I, Bruttini M, Mari F, Renieri A. Type-IV collagen related diseases. *J Nephrol.* 2003;16(2):314–316.
5. Barker DF, et al. Identification of mutations in the COL4A5 collagen gene in Alport syndrome. *Science.* 1990;248(4960):1224–1227.
6. Lemmink HH, et al. Mutations in the type IV collagen alpha 3 (COL4A3) gene in autosomal recessive Alport syndrome. *Hum Mol Genet.* 1994;3(8):1269–1273.
7. Mochizuki T, et al. Identification of mutations in the alpha 3(IV) and alpha 4(IV) collagen genes in autosomal recessive Alport syndrome. *Nat Genet.* 1994;8(1):77–81.
8. Zoja C, Morigi M, Benigni A, Remuzzi G. Genetics of rare diseases of the kidney: learning from mouse models. *Cytogenet Genome Res.* 2004;

105(2–4):479–484.

9. Kalluri R, Shield CF, Todd P, Hudson BG, Neilson EG. Isoform switching of type IV collagen is developmentally arrested in X-linked Alport syndrome leading to increased susceptibility of renal basement membranes to endoproteolysis. *J Clin Invest*. 1997;99(10):2470–2478.

10. Massague J, Chen YG. Controlling TGF-beta signaling. *Genes Dev*. 2000;14(6):627–644.

11. Helder MN, et al. Expression pattern of osteogenic protein-1 (bone morphogenetic protein-7) in human and mouse development. *J Histochem Cytochem*. 1995;43(10):1035–1044.

12. Vukicevic S, et al. Osteogenic protein-1 (bone morphogenetic protein-7) reduces severity of injury after ischemic acute renal failure in rat. *J Clin Invest*. 1998;102(1):202–214.

13. Zeisberg M, et al. Bone morphogenic protein-7 inhibits progression of chronic renal fibrosis associated with two genetic mouse models. *Am J Physiol Renal Physiol*. 2003;285(6):F1060–F1067.

14. Zeisberg M, et al. BMP-7 counteracts TGF-beta1-induced epithelial-to-mesenchymal transition and reverses chronic renal injury. *Nat Med*. 2003;9(7):964–968.

15. Morrissey J, Hruska K, Guo G, Wang S, Chen Q, Klahr S. Bone morphogenetic protein-7 improves renal fibrosis and accelerates the return of renal function. *J Am Soc Nephrol*. 2002;13(Suppl 1):S14–S21.

16. Hruska KA. Treatment of chronic tubulointerstitial disease: a new concept. *Kidney Int*. 2002; 61(5):1911–1922.

17. Hruska KA, Guo G, Wozniak M, Martin D, Miller S, Liapis H, Loveday K, Klahr S, Sampath TK, Morrissey J. Osteogenic protein-1 prevents renal fibrogenesis associated with ureteral obstruction. *Am J Physiol Renal Physiol*. 2000;279(1):F130–F143.

18. Hruska KA, Saab G, Chaudhary LR, Quinn CO, Lund RJ, Surendran K. Kidney-bone, bone-kidney, and cell-cell communications in renal osteodystrophy. *Semin Nephrol*. 2004;24(1):25–38.

19. Zeisberg M, Shah AA, Kalluri R. Bone morphogenic protein-7 induces mesenchymal to epithelial transition in adult renal fibroblasts and facilitates regeneration of injured kidney. *J Biol Chem*. 2005;280(9):8094–8100.

20. Wang S, de Caestecker M, Kopp J, Mitu G, Lapage J, Hirschberg R. Renal bone morphogenetic protein-7 protects against diabetic nephropathy. *J Am Soc Nephrol*. 2006;17(9):2504–2512.

21. Reddi AH. Interplay between bone morphogenetic proteins and cognate binding proteins in bone and cartilage development: noggin, chordin and DAN. *Arthritis Res*. 2001;3(1):1–5.

22. Yanagita M. BMP antagonists: Their roles in development and involvement in pathophysiology. *Cytokine Growth Factor Rev*. 2005;16(3):309–317.

23. Yanagita M. Modulator of bone morphogenetic protein activity in the progression of kidney diseases. *Kidney Int*. 2006; 70(6):989–993.

24. Eddy AA. Ramping up endogenous defences against chronic kidney disease. *Nephrol Dial Transplant*. 2006;21(5):1174–1177.

25. Yanagita M, et al. USAG-1: a bone morphogenetic protein antagonist abundantly expressed in the kidney. *Biochem Biophys Res Commun*. 2004; 316(2):490–500.

26. Tanaka M, et al. Expression of BMP-7 and USAG-1 (a BMP antagonist) in kidney development and injury. *Kidney Int*. 2008;73(2):181–191.

27. Yanagita M, et al. Uterine sensitization-associated gene-1 (USAG-1), a novel BMP antagonist expressed in the kidney, accelerates tubular injury. *J Clin Invest*. 2006;116(1):70–79.

28. Sayers R, Kalluri R, Rodgers KD, Shield CF, Meehan DT, Cosgrove D. Role for transforming growth factor-beta1 in alport renal disease progression.

Kidney Int. 1999;56(5):1662–1673.

29. Rao VH, et al. Role for macrophage metalloelastase in glomerular basement membrane damage associated with alport syndrome. *Am J Pathol*. 2006;169(1):32–46.

30. Schmierer B, Hill CS. TGFbeta-SMAD signal transduction: molecular specificity and functional flexibility. *Nat Rev Mol Cell Biol*. 2007;8(12):970–982.

31. Wang SN, Lapage J, Hirschberg R. Loss of tubular bone morphogenetic protein-7 in diabetic nephropathy. *J Am Soc Nephrol*. 2001;12(11):2392–2399.

32. Daly AC, Randall RA, Hill CS. Transforming growth factor beta-induced Smad1/5 phosphorylation in epithelial cells is mediated by novel receptor complexes and is essential for anchorage-independent growth. *Mol Cell Biol*. 2008;28(22):6889–6902.

33. Goumans MJ, et al. Activin receptor-like kinase (ALK)1 is an antagonistic mediator of lateral TGF-beta/ALK5 signaling. *Mol Cell*. 2003;12(4):817–828.

34. Pannu J, Nakerakanti S, Smith E, ten Dijke P, Trojanowska M. Transforming growth factor-beta receptor type I-dependent fibrogenic gene program is mediated via activation of Smad1 and ERK1/2 pathways. *J Biol Chem*. 2007;282(14):10405–10413.

35. Kim JH, Ryu KH, Jung KW, Han CK, Kwak WJ, Cho YB. SKI306X suppresses cartilage destruction and inhibits the production of matrix metalloproteinase in rabbit joint cartilage explant culture. *J Pharmacol Sci*. 2005;98(3):298–306.

36. Kaneko Y, et al. Macrophage metalloelastase as a major factor for glomerular injury in anti-glomerular basement membrane nephritis. *J Immunol*. 2003;170(6):3377–3385.

37. Vos CM, van Haastert ES, de Groot CJ, van der Valk P, de Vries HE. Matrix metalloproteinase-12 is expressed in phagocytotic macrophages in active multiple sclerosis lesions. *J Neuroimmunol*. 2003;138(1–2):106–114.

38. Eddy AA. Molecular insights into renal interstitial fibrosis. *J Am Soc Nephrol*. 1996;7(12):2495–2508.

39. van Kooten C, Daha MR, van Es LA. Tubular epithelial cells: A critical cell type in the regulation of renal inflammatory processes. *Exp Nephrol*. 1999;7(5–6):429–437.

40. Zeisberg M, et al. Stage-specific action of matrix metalloproteinases influences progressive hereditary kidney disease. *PLoS Med*. 2006;3(4):e100.

41. Mitu GM, Wang S, Hirschberg R. BMP7 is a podocyte survival factor and rescues podocytes from diabetic injury. *Am J Physiol Renal Physiol*. 2007;293(5):F1641–F1648.

42. De Petris L, Hruska KA, Chiechio S, Liapis H. Bone morphogenetic protein-7 delays podocyte injury due to high glucose. *Nephrol Dial Transplant*. 2007;22(12):3442–3450.

43. Otani H, et al. Antagonistic effects of bone morphogenetic protein-4 and -7 on renal mesangial cell proliferation induced by aldosterone through MAPK activation. *Am J Physiol Renal Physiol*. 2007;292(5):F1513–F1525.

44. Chan WL, Leung JC, Chan LY, Tam KY, Tang SC, Lai KN. BMP-7 protects mesangial cells from injury by polymeric IgA. *Kidney Int*. 2008;74(8):1026–1039.

45. Wang S, Hirschberg R. BMP7 antagonizes TGF-beta-dependent fibrogenesis in mesangial cells. *Am J Physiol Renal Physiol*. 2003;284(5):F1006–F1013.

46. Gould SE, Day M, Jones SS, Dorai H. BMP-7 regulates chemokine, cytokine, and hemodynamic gene expression in proximal tubule cells. *Kidney Int*. 2002;61(1):51–60.

47. Bell PD, Lapointe JY, Peti-Peterdi J. Macula densa cell signaling. *Annu Rev Physiol*. 2003;65:481–500.

48. Barajas L. Anatomy of the juxtaglomerular apparatus. *Am J Physiol*. 1979;237(5):F333–F343.

49. Lapointe JY, Laamarti A, Bell PD. Ionic transport in macula densa cells. *Kidney Int Suppl*. 1998; 67:S58–S64.

50. Navar LG, Inscho EW, Majid SA, Imig JD, Harrison-Bernard LM, Mitchell KD. Paracrine regulation of the renal microcirculation. *Physiol Rev*. 1996;76(2):425–536.

51. Navar LG, Ploth DW, Bell PD. Distal tubular feedback control of renal hemodynamics and autoregulation. *Annu Rev Physiol*. 1980;42:557–571.

52. Schnermann J, et al. Tubuloglomerular feedback: new concepts and developments. *Kidney Int Suppl*. 1998;67:S40–S45.

53. Tojo A, Onozato ML, Fujita T. Role of macula densa neuronal nitric oxide synthase in renal diseases. *Med Mol Morphol*. 2006;39(1):2–7.

54. Ren Y, Carretero OA, Garvin JL. Role of mesangial cells and gap junctions in tubuloglomerular feedback. *Kidney Int*. 2002;62(2):525–531.

55. Hugo C, Shankland SJ, Bowen-Pope DF, Couser WG, Johnson RJ. Extraglomerular origin of the mesangial cell after injury. A new role for the juxtaglomerular apparatus. *J Clin Invest*. 1997;100(4):786–794.

56. Gross O, et al. Preemptive ramipril therapy delays renal failure and reduces renal fibrosis in COL4A3-knockout mice with Alport syndrome. *Kidney Int*. 2003;63(2):438–446.

57. Koepke ML, Weber M, Schulze-Lohoff E, Beirowski B, Segerer S, Gross O. Nephroprotective effect of the HMG-CoA-reductase inhibitor cerivastatin in a mouse model of progressive renal fibrosis in Alport syndrome. *Nephrol Dial Transplant*. 2007;22(4):1062–1069.

58. Sugimoto H, Mundel TM, Sund M, Xie L, Cosgrove D, Kalluri R. Bone-marrow-derived stem cells repair basement membrane collagen defects and reverse genetic kidney disease. *Proc Natl Acad Sci U S A*. 2006;103(19):7321–7326.

59. Floege J, Kunter U, Weber M, Gross O. Bone marrow transplantation rescues Alport mice. *Nephrol Dial Transplant*. 2006;21(10):2721–2723.

60. Prodromidi EI, et al. Bone marrow-derived cells contribute to podocyte regeneration and amelioration of renal disease in a mouse model of Alport syndrome. *Stem Cells*. 2006;24(11):2448–2455.

61. Katayama K, et al. Irradiation prolongs survival of Alport mice. *J Am Soc Nephrol*. 2008;19(9):1692–1700.

62. Cosgrove D, et al. Collagen COL4A3 knockout: a mouse model for autosomal Alport syndrome. *Genes Dev*. 1996;10(23):2981–2992.

63. Yanagita M, et al. Gas6 regulates mesangial cell proliferation through Axl in experimental glomerulonephritis. *Am J Pathol*. 2001;158(4):1423–1432.

64. Kawachi H, Koike H, Kurihara H, Sakai T, Shimizu F. Cloning of rat homologue of podocin: expression in proteinuric states and in developing glomeruli. *J Am Soc Nephrol*. 2003;14(1):46–56.

65. Sado Y, et al. Establishment by the rat lymph node method of epitope-defined monoclonal antibodies recognizing the six different alpha chains of human type IV collagen. *Histochem Cell Biol*. 1995;104(4):267–275.

66. Valenzuela DM, et al. High-throughput engineering of the mouse genome coupled with high-resolution expression analysis. *Nat Biotechnol*. 2003;21(6):652–659.

67. Yanagita M, et al. Gas6 induces mesangial cell proliferation via latent transcription factor STAT3. *J Biol Chem*. 2001;276(45):42364–42369.

68. MacKay K, Striker LJ, Elliot S, Pinkert CA, Brinster RL, Striker GE. Glomerular epithelial, mesangial, and endothelial cell lines from transgenic mice. *Kidney Int*. 1988;33(3):677–684.

69. Rodgers KD, et al. Monocytes may promote myofibroblast accumulation and apoptosis in Alport renal fibrosis. *Kidney Int*. 2003;63(4):1338–1355.

70. Lories RJ, Derese I, Luyten FP. Modulation of bone morphogenetic protein signaling inhibits the onset and progression of ankylosing enthesitis. *J Clin Invest*. 2005;115(6):1571–1579.